2018

Birefringence Microscopy with Magnetic-Field Aligned Multiferroic Janus Nanofibers

Yu-Chun Yeh
University of South Carolina

Birefringence Microscopy with Magnetic-Field Aligned Multiferroic Janus Nanofibers

by

Yu-Chun Yeh

Bachelor of Science
National Kaohsiung Normal University, 2012

Submitted in Partial Fulfillment of the Requirements

For the Degree of Master of Science in

Physics

College of Arts and Sciences

University of South Carolina

2018

Accepted by:

Thomas M. Crawford, Director of Thesis

Yanwen Wu, Reader

Cheryl L. Addy, Vice Provost and Dean of the Graduate School

ABSTRACT

Multiferroic Janus nanofibers consisting of barium titanate ($BaTiO_3$) and cobalt ferrite ($CoFe_2O_4$) have the magnetoelectric effect between piezoelectric and magnetostrictive phases. By applying an external magnetic field on Janus nanofibers, the dipole moment in piezoelectric phase would be formed and produce the electric field. Since poly(N-vinylcarbazole) (PVK) polymer has anisotropic property, the birefringence can be induced by the electric field. We generalize the magnetic field-birefringence quadratic equation and coupling constant for PVK polymer with Janus nanofibers. Birefringence microscopy is used to observe the PVK birefringence under an external magnetic field from 0 to 2500 Oe. The numerical results show that the birefringence variation of the fourth digit after the dot can be obviously detected by our microscope for the distance within 15 μm between two nanofibers in PVK polymer.

TABLE OF CONTENTS

List of Tables

List of Figures

Chapter 1

Introduction and Motivation

Magnetoelectric multiferroics have been studied as the coupling interaction between piezoelectric and magnetostrictive materials. The magnetoelectric effect is the phenomenon in multiferroic materials that an electric polarization is produced by applying an external magnetic field or a magnetization is produced by applying an external electric field. Janus nanofibers (Figure 1.1) manufactured by electrospinning method [1] have two different semi-cylindrical phases containing barium titanate ($BaTiO_3$) and cobalt ferrite ($CoFe_2O_4$). In order to understand the properties and applications of multiferroic materials, we can use Janus nanofibers and poly(N-vinylcarbazole) (PVK) polymer to make samples and cure them with the constant magnetic field. While curing, Janus nanofibers form long-chain alignment along the field direction. Due to the magnetoelectric effect, the piezoelectric phase is polarized and the electric field of dipole is produced from $BaTiO_3$. According to Kerr electro-optic effect, the electric field can induce birefringence in a PVK polymer [2]. A polarized light microscopy is used to detect the birefringent behavior under an applied magnetic field ranging from 0 to 2500 Oe. Chaper 2 includes theoretical calculation for magnetic field-birefringence in a PVK solution with Janus nanofibers using a Green's function method, as well as [3][4] and the numerical results for PVK and other polymers. In Chapter 3, we will discuss the birefringence spectroscopy and simulation data analysis. Conclusion and suggested future work are included in Chapter 4.

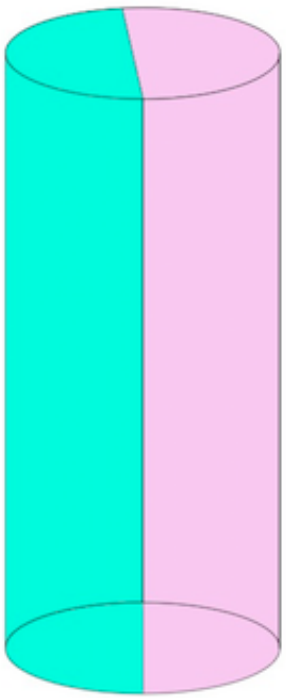

Figure 1.1: Janus nanofiber consists of $BaTiO_3$ (left side) and $CoFe_2O_4$ (right side).

Chapter 2

Theory

Janus nanofibers exhibit the direct magnetoelectric effect which couples magnetostrictive and piezoelectric properties. In $CoFe_2O_4$, there are many randomly oriented domains (Figure 2.1). When an external magnetic field is applied to the system, each domain produces torque $\vec{N} = \vec{m} \times \vec{B}$, which tries to rotate the domains along the field direction. Due to the effect of orientation, a strain field is created that change elongates the composite in Figure 2.2, an effect called magnetostriction [3][5].

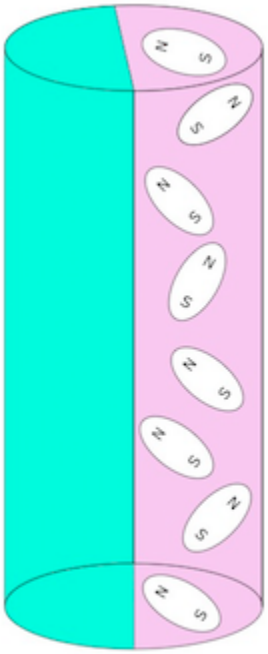

Figure 2.1: Randomly oriented domains exist in $CoFe_2O_4$.

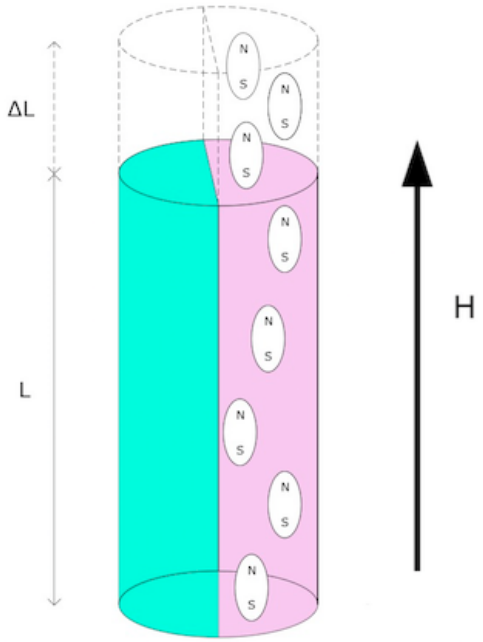

Figure 2.2: The strain field forces the Janus nanofiber to extend the length.

Since the stress acts upon the barium titanate, the piezoelectric domains are polarized and an electric dipole moment is formed in Figure 2.3.

To understand the magnetoelectric coupling in multiferroic composites, the Green's function method by Ce-Wen Nan [3][4] can be used to get an effective magnetoelectric coefficient for Janus nanofibers. Birefringence can be induced in PVK by an electric field. In Sec. 2.1, we obtain a quadratic equation for magnetic field-birefringence and the coupling constant for a PVK solution with Janus nanofibers.

2.1 Magnetic field-birefringence coupling equation

For multiferroic composites, the constitutive equations for coupling magneto-mechanical-electric interactions can be written as

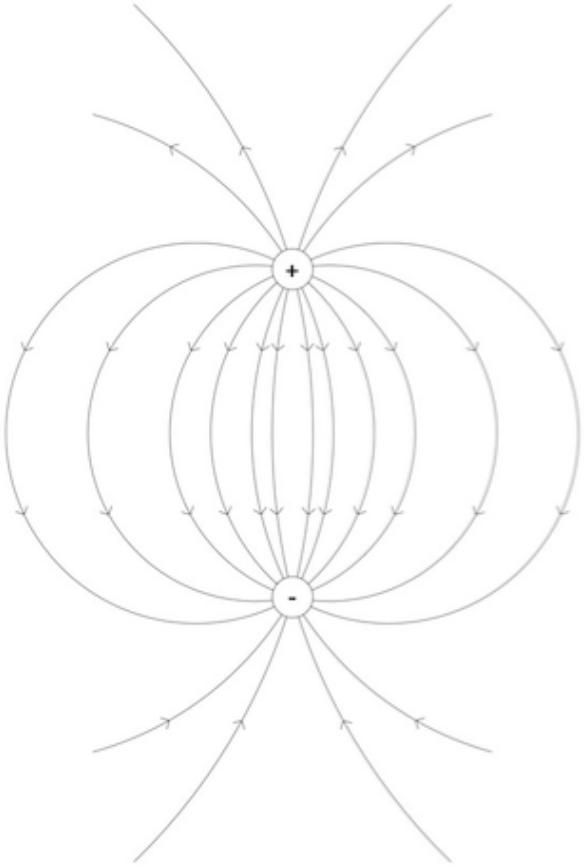

Figure 2.3: The dipole moment in $BaTiO_3$ creates an electric field as shown.

$$\begin{aligned} \sigma_{ij} &= C_{ijkl}s_{kl} - e_{lij}E_l - q_{lij}H_l, \\ D_i &= e_{ikl}s_{kl} + \varepsilon_{il}E_l + \alpha_{il}H_l, \\ B_i &= q_{ikl}s_{kl} + \alpha_{li}E_l + \mu_{il}H_l, \end{aligned} \tag{2.1}$$

where σ, C, s, e, q, E, D, B, H, ε, μ, and α are stress, stiffness, strain, piezoelectric coefficient, piezomagnetic coefficient, electric field, electric displacement, magnetic induction, magnetic field, dielectric constant, permeability, and magnetoelectric coefficient, respectively.

Janus nanofibers which have two different phases are nonhomogeneous materials. In order to consider the statistical combination of magnetostrictive and piezoelectric

properties at a macroscopic level [6], we can take average of constitutive equations as

$$\begin{aligned} < \sigma_{ij} > &= C^*_{ijkl} < s_{kl} > - e^*_{lij} < E_l > - q^*_{lij} < H_l >, \\ < D_i > &= e^*_{ikl} < s_{kl} > + \varepsilon^*_{il} < E_l > + \alpha^*_{il} < H_l >, \\ < B_i > &= q^*_{ikl} < s_{kl} > + \alpha^*_{li} < E_l > + \mu^*_{il} < H_l > . \end{aligned} \tag{2.2}$$

The constitutive coefficients C(x), ε(x), and μ(x) can be wriiten by perturbation theory [6] as

$$\begin{aligned} C(x) &= C^0 + C'(x), \\ \varepsilon(x) &= \varepsilon^0 + \varepsilon'(x), \\ \mu(x) &= \mu^0 + \mu'(x), \end{aligned} \tag{2.3}$$

where C^0, ε^0, and μ^0 are homogeneous terms and the notations of prime represent fluctuations.

Consider the homogeneous boundary conditions on the external surface S and the elastic displacement, electric potential, and magnetic potential are

$$\begin{aligned} u_i(S) &= u^0_i = s^0_{ij} x_j, \\ \phi(S) &= \phi^0 = -E^0_i x_i, \\ \mathscr{V}(S) &= \mathscr{V}^0 = -H^0_i x_i. \end{aligned} \tag{2.4}$$

In static equlibrium, the differentiation of constitutive equations (2.1) are zero:

$$\begin{aligned} \frac{\partial \sigma_{ij}(x)}{\partial x_j} &= 0, \\ \frac{\partial D_i(x)}{\partial x_i} &= 0, \\ \frac{\partial B_i(x)}{\partial x_i} &= 0. \end{aligned} \tag{2.5}$$

Now, we substitute equations (2.1) and (2.3) into equation (2.5) and obtain

$$
\begin{aligned}
C^0_{ijkl}\frac{\partial s_{kl}}{\partial x_j} + \frac{\partial}{\partial x_j}(C'_{ijkl}s_{kl} - e_{nij}E_n - q_{nij}H_n) &= 0, \\
\varepsilon^0_{in}\frac{\partial E_n}{\partial x_i} + \frac{\partial}{\partial x_i}(e_{ijn}s_{jn} + \varepsilon'_{in}E_n + \alpha_{in}H_n) &= 0, \\
\mu^0_{in}\frac{\partial H_n}{\partial x_i} + \frac{\partial}{\partial x_i}(q_{ijn}s_{jn} + \alpha_{in}E_n + \mu'_{in}H_n) &= 0.
\end{aligned} \tag{2.6}
$$

Take the derivative of s_{kl}, E_n and H_n and the equations (2.6) can be written as

$$
\begin{aligned}
C^0_{ijkl}\frac{\partial^2 u_k}{\partial x_j \partial x_l} + \frac{\partial}{\partial x_j}(C'_{ijkl}s_{kl} - e_{nij}E_n - q_{nij}H_n) &= 0, \\
\varepsilon^0_{in}\frac{\partial^2 \phi}{\partial x_i \partial x_n} + \frac{\partial}{\partial x_i}(e_{ijn}s_{jn} + \varepsilon'_{in}E_n + \alpha_{in}H_n) &= 0, \\
\mu^0_{in}\frac{\partial^2 \mathscr{V}}{\partial x_i \partial x_n} + \frac{\partial}{\partial x_i}(q_{ijn}s_{jn} + \alpha_{in}E_n + \mu'_{in}H_n) &= 0.
\end{aligned} \tag{2.7}
$$

We integrate the elastic displacement, electric potential, and magnetic potential twice and the solutions can be described as

$$
\begin{aligned}
u_k(x) &= u^0_k + \int g^u_{ki}(x,x')\frac{\partial}{\partial x'_j}(C'_{ijkl}s_{kl} - e_{nij}E_n - q_{nij}H_n)dx', \\
\phi(x) &= \phi^0 + \int g^\phi(x,x')\frac{\partial}{\partial x'_i}(e_{ijn}s_{jn} + \varepsilon'_{in}E_n + \alpha_{in}H_n)dx', \\
\mathscr{V}(x) &= \mathscr{V}^0 + \int g^{\mathscr{V}}(x,x')\frac{\partial}{\partial x'_i}(q_{ijn}s_{jn} + \alpha_{in}E_n + \mu'_{in}H_n)dx',
\end{aligned} \tag{2.8}
$$

where $g^u_{ki}(x,x')$, $g^\phi(x,x')$, and $g^{\mathscr{V}}(x,x')$ are elastic displacement Green's function, electric potential Green's function, and magnetic potential Green's function [4].

If we differentiate equations (2.8) and use integration by parts to get strain, electric field, and magnetic field, then

$$
\begin{aligned}
s(x) &= s^0 + \int \widetilde{G}^u(x,x')[C'(x')s(x') - e^T(x')E(x') - q^T(x')H(x')]dx', \\
E(x) &= E^0 + \int \widetilde{G}^\phi(x,x')[e(x')s(x') + \varepsilon'(x')E(x') + \alpha(x')H(x')]dx', \\
H(x) &= H^0 + \int \widetilde{G}^\mu(x,x')[q(x')s(x') + \alpha^T(x')E(x') + \mu'(x')H(x')]dx',
\end{aligned} \tag{2.9}
$$

where $\widetilde{G}^u(x,x')$, $\widetilde{G}^\phi(x,x')$, and $\widetilde{G}^\mu(x,x')$ are modified elastic displacement Green's function, electric potential Green's function, and magnetic potential Green's function [4]. The superscript T stands for the transpose of matrix.

The equations (2.9) can be described in operator notation:

$$\begin{aligned} s(x) &= s^0 + G^u(C's - e^T E - q^T H), \\ E(x) &= E^0 + G^\phi(es + \varepsilon' E + \alpha H), \\ H(x) &= H^0 + G^\mu(qs + \alpha^T E + \mu' H). \end{aligned} \tag{2.10}$$

Write equations (2.10) in matrix form:

$$\begin{aligned} \begin{bmatrix} s \\ E \\ H \end{bmatrix} &= \begin{bmatrix} s^0 \\ E^0 \\ H^0 \end{bmatrix} + \begin{bmatrix} G^u & 0 & 0 \\ 0 & G^\phi & 0 \\ 0 & 0 & G^\gamma \end{bmatrix} \begin{bmatrix} C' & -e^T & -q^T \\ e & \varepsilon' & \alpha \\ q & \alpha^T & \mu' \end{bmatrix} \begin{bmatrix} s \\ E \\ H \end{bmatrix} \\ &= \begin{bmatrix} s^0 \\ E^0 \\ H^0 \end{bmatrix} + \begin{bmatrix} G^u C' & -G^u e^T & -G^u q^T \\ G^\phi e & G^\phi \varepsilon' & G^\phi \alpha \\ G^\gamma q & G^\gamma \alpha^T & G^\gamma \mu' \end{bmatrix} \begin{bmatrix} s \\ E \\ H \end{bmatrix}. \end{aligned} \tag{2.11}$$

If we move the field matrix to the left side and multiply the inverse of Green's function matrix on both sides, then we get

$$\begin{bmatrix} s \\ E \\ H \end{bmatrix} = \begin{bmatrix} T^{11} & T^{12} & T^{13} \\ T^{21} & T^{22} & T^{23} \\ T^{31} & T^{32} & T^{33} \end{bmatrix} \begin{bmatrix} s^0 \\ E^0 \\ H^0 \end{bmatrix}, \tag{2.12}$$

where T^{ij} is the T-type tensor [3].

The constitutive equations (2.1) can be written in matrix form:

$$\begin{bmatrix} \sigma \\ D \\ B \end{bmatrix} = \begin{bmatrix} C & -e^T & -q^T \\ e & \varepsilon & \alpha \\ q & \alpha^T & \mu \end{bmatrix} \begin{bmatrix} T^{11} & T^{12} & T^{13} \\ T^{21} & T^{22} & T^{23} \\ T^{31} & T^{32} & T^{33} \end{bmatrix} \begin{bmatrix} s^0 \\ E^0 \\ H^0 \end{bmatrix}$$

$$= \begin{bmatrix} CT^{11} - e^T T^{21} - q^T T^{31} & CT^{12} - e^T T^{22} - q^T T^{32} & CT^{13} - e^T T^{23} - q^T T^{33} \\ eT^{11} + \varepsilon T^{21} + \alpha T^{31} & eT^{12} + \varepsilon T^{22} + \alpha T^{32} & eT^{13} + \varepsilon T^{23} + \alpha T^{33} \\ qT^{11} + \alpha^T T^{21} + \mu T^{31} & qT^{12} + \alpha^T T^{22} + \mu T^{32} & qT^{13} + \alpha^T T^{23} + \mu T^{33} \end{bmatrix} \begin{bmatrix} s^0 \\ E^0 \\ H^0 \end{bmatrix}$$

$$= \begin{bmatrix} R^{11} & R^{12} & R^{13} \\ R^{21} & R^{22} & R^{23} \\ R^{31} & R^{32} & R^{33} \end{bmatrix} \begin{bmatrix} s^0 \\ E^0 \\ H^0 \end{bmatrix}, \tag{2.13}$$

where R^{ij} represents the matrix element.

We take the average of matrix in equation (2.13) and then

$$\begin{bmatrix} <\sigma> \\ <D> \\ <B> \end{bmatrix} = \begin{bmatrix} <R^{11}> & <R^{12}> & <R^{13}> \\ <R^{21}> & <R^{22}> & <R^{23}> \\ <R^{31}> & <R^{32}> & <R^{33}> \end{bmatrix} \begin{bmatrix} <s^0> \\ <E^0> \\ <H^0> \end{bmatrix}. \tag{2.14}$$

Now, the averaged constitutive equations (2.2) can be written in matrix form:

$$\begin{bmatrix} <\sigma> \\ <D> \\ <B> \end{bmatrix} = \begin{bmatrix} C^* & -e^{T^*} & -q^{T^*} \\ e^* & \varepsilon^* & \alpha^* \\ q^* & \alpha^{T^*} & \mu^* \end{bmatrix} \begin{bmatrix} <s> \\ <E> \\ <H> \end{bmatrix}$$

$$= \begin{bmatrix} C^* & -e^{T^*} & -q^{T^*} \\ e^* & \varepsilon^* & \alpha^* \\ q^* & \alpha^{T^*} & \mu^* \end{bmatrix} \begin{bmatrix} <T^{11}> & <T^{12}> & <T^{13}> \\ <T^{21}> & <T^{22}> & <T^{23}> \\ <T^{31}> & <T^{32}> & <T^{33}> \end{bmatrix} \begin{bmatrix} <s^0> \\ <E^0> \\ <H^0> \end{bmatrix}$$

$$= \begin{bmatrix} <U^{11}> & <U^{12>} & <U^{13}> \\ <U^{21}> & <U^{22>} & <U^{23}> \\ <U^{31}> & <U^{32}> & <U^{33}> \end{bmatrix} \begin{bmatrix} <s^0> \\ <E^0> \\ <H^0> \end{bmatrix}, \tag{2.15}$$

where $<U^{ij}>$ is the averaged element of matrix.

Compare the matrix elements $<R^{23}>$ and $<U^{23}>$ from equations (2.14) and

(2.15) and obtain

$$< eT^{13} + \varepsilon T^{23} + \alpha T^{33} >= e^* < T^{13} > + \varepsilon^* < T^{23} > + \alpha^* < T^{33} > . \tag{2.16}$$

Owing to the fact that the magnetoelectric effect doesn't exist in both individual phases, $\alpha = 0$. The piezomagnetic effect doesn't exist in piezoelectric phase, so $q = 0$ and T^{23} can be neglected [3].

The effective magnetoelectric coefficient can be described as

$$\alpha^* =< (e - e^*)T^{13} >< T^{33} >^{-1}, \tag{2.17}$$

where α^* is nonzero for multiferroic composites.

The effective electric polarization of barium titanate is

$$p^* = \alpha^* < H > . \tag{2.18}$$

The matrix form of equation (2.18) is

$$\begin{bmatrix} {p_1}^* \\ {p_2}^* \\ {p_3}^* \end{bmatrix} = \begin{bmatrix} \alpha_{11}^* & \alpha_{12}^* & \alpha_{13}^* \\ \alpha_{21}^* & \alpha_{22}^* & \alpha_{23}^* \\ \alpha_{31}^* & \alpha_{32}^* & \alpha_{33}^* \end{bmatrix} \begin{bmatrix} < H_1 > \\ < H_2 > \\ < H_3 > \end{bmatrix} . \tag{2.19}$$

Since we apply an external magnetic field along z-axis in Figure 2.4, $< H_1 >$ and $< H_2 >$ are zeros and the effective polarization of z-direction would be

$$p_3^* = \alpha_{33}^* < H_3 >= \alpha_{33}^* H_3^{ext}, \tag{2.20}$$

where H_3^{ext} stands for the external magnetic field.

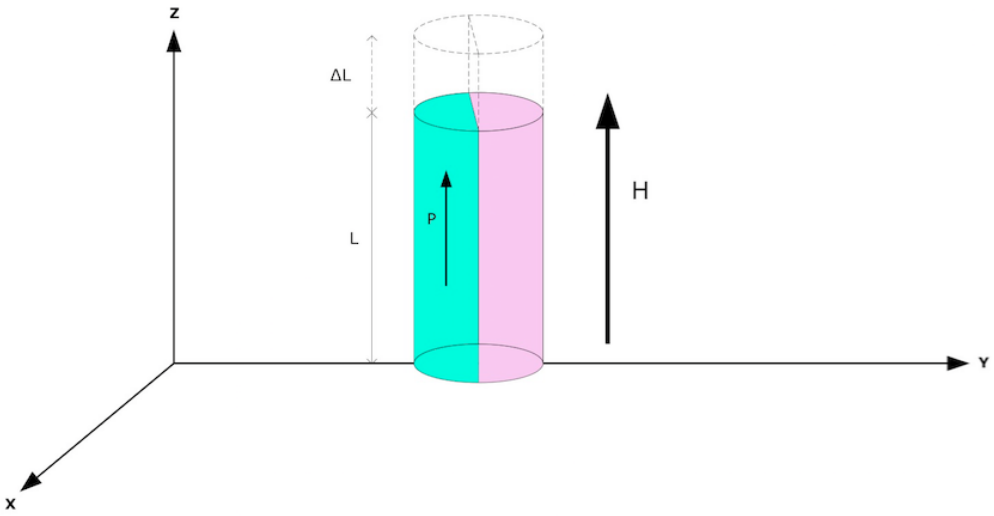

Figure 2.4: An external magnetic field is applied to a Janus nanofiber in the z-direction.

For the 1-3 type magnetostrictive-piezoelectric composite, the effective magnetoelectric coefficient α_{33}^* obtained by non-self-consistent approximation (NSCA) [3][5] can be described as

$$\alpha_{33}^* = -\frac{f(1-f)q_{31}e_{31}}{{}^m k + {}^p m + f({}^p k - {}^m k)}, \tag{2.21}$$

where $k = \frac{C11+C12}{2}$, $m = \frac{C11-C12}{2}$, and f is the volume fraction of the magnetostrictive phase. Table 2.1 shows the parameters of piezoelectric and magnetostrictive phases [3].

Since the polarization is regarded as the combination of many tiny dipole moments in $BaTiO_3$, the dipole moment in Figure 2.5 could be

$$p_{dip} = p_3^* V, \tag{2.22}$$

where V is the volume of piezoelectric phase.

Table 2.1: Parameters of $BaTiO_3$ and $CoFe_2O_4$.

	$BaTiO_3$	$CoFe_2O_4$
C_{11} (GPa)	166.2	286.0
C_{12} (GPa)	76.5	173.0
C_{13} (GPa)	77.4	170.5
C_{33} (GPa)	161.4	269.5
$\varepsilon_{33}/\varepsilon^0$	1350	10
μ_{33}/μ^0	8	125
e_{31} (C/m^2)	-4.22	0
e_{33} (C/m^2)	18.6	0
q_{31} (N/Am)	0	580.3
q_{33} (N/Am)	0	699.7

The dipole potential becomes

$$V_{dip}(r,\theta) = \frac{\hat{r}\cdot\vec{p}_{dip}}{4\pi\epsilon_0 r^2}. \tag{2.23}$$

To calculate the electric field, we take the negative gradient of V_{dip} in spherical coordinates:

$$\begin{aligned}
\vec{E}_{dip}(r,\theta) &= \vec{E}_{r_{dip}} + \vec{E}_{\theta_{dip}} + \vec{E}_{\phi_{dip}} \\
&= -\nabla V_{dip} \\
&= -(\tfrac{\partial V}{\partial r}\hat{r} + \tfrac{1}{r}\tfrac{\partial V}{\partial \theta}\hat{\theta} + \tfrac{1}{r\sin\theta}\tfrac{\partial V}{\partial \phi}\hat{\phi}) \\
&= -(-\tfrac{-2p_{dip}\cos\theta}{4\pi\epsilon_0 r^3}\hat{r} - \tfrac{p_{dip}\sin\theta}{4\pi\epsilon_0 r^3}\hat{\theta} + 0 \\
&= \tfrac{p_{dip}}{4\pi\epsilon_0 r^3}(-2\cos\theta\hat{r} + \sin\theta\hat{\theta}).
\end{aligned} \tag{2.24}$$

Assume that the other fiber is next to the original one and the electric fields from both fibers should be

$$\begin{aligned}
\vec{E}_{1_{dip}} &= \tfrac{p_{1_{dip}}}{4\pi\epsilon_0 {r_1}^3}(-2\cos\theta_1\hat{r} + \sin\theta_1\hat{\theta}), \\
\vec{E}_{2_{dip}} &= \tfrac{p_{2_{dip}}}{4\pi\epsilon_0 {r_2}^3}(-2\cos\theta_2\hat{r} + \sin\theta_2\hat{\theta}).
\end{aligned} \tag{2.25}$$

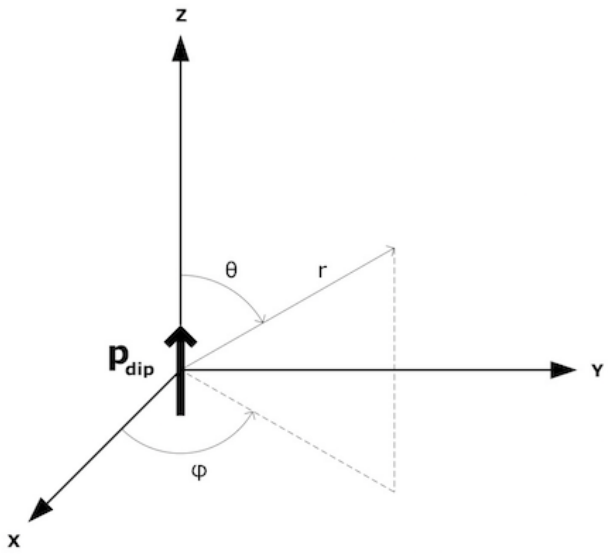

Figure 2.5: The dipole moment p_{dip} points in the z-direction.

Let's consider the case of the midpoint between both fibers. Since $\theta_1 = \theta_2 = 180^o$, the total electric field in Figure 2.6 would point along the negative z-direction:

$$\begin{aligned}
\vec{E}_{total} &= -\frac{2}{4\pi\epsilon_0}\left(\frac{P_{1_{dip}}}{{r_1}^3} + \frac{P_{2_{dip}}}{{r_2}^3}\right)\hat{r} \\
&= -\frac{2}{4\pi\epsilon_0}\left(\frac{P_{1_{dip}}}{{r_1}^3} + \frac{P_{2_{dip}}}{{r_1}^3}\right)\hat{r} \\
&= -\frac{2}{4\pi\epsilon_0}\frac{(P_{1_{dip}}+P_{2_{dip}})}{{r_1}^3}\hat{r} \\
&= -\frac{1}{2\pi\epsilon_0}\frac{\alpha^*_{33}H_3^{ext}(V_1+V_2)}{{r_1}^3}\hat{r} \\
&= -\frac{1}{2\pi\epsilon_0}\frac{\alpha^*_{33}H_3^{ext}(V_1+V_2)}{(\frac{d}{2})^3}\hat{r} \\
&= -\frac{4}{\pi\epsilon_0}\frac{\alpha^*_{33}H_3^{ext}(V_1+V_2)}{d^3}\hat{r} \\
&= -\frac{4}{\pi\epsilon_0}\frac{\alpha^*_{33}(V_1+V_2)}{d^3}\frac{250}{\pi}H\hat{r} \\
&= -\frac{1000\alpha^*_{33}(V_1+V_2)}{\pi^2\epsilon_0 d^3}H\hat{r},
\end{aligned} \tag{2.26}$$

where d is the distance between both fibers. The unit conversion of magnetic field is $H_3^{ext} = H(Oe) = \frac{1000}{4\pi}H(A/m) = \frac{250}{\pi}H(A/m)$.

The birefringence of PVK polymer [2] is

$$\Delta n = n_e - n_o = (4.96 \times 10^{-7})E^2 + 5.12 \times 10^{-4}. \tag{2.27}$$

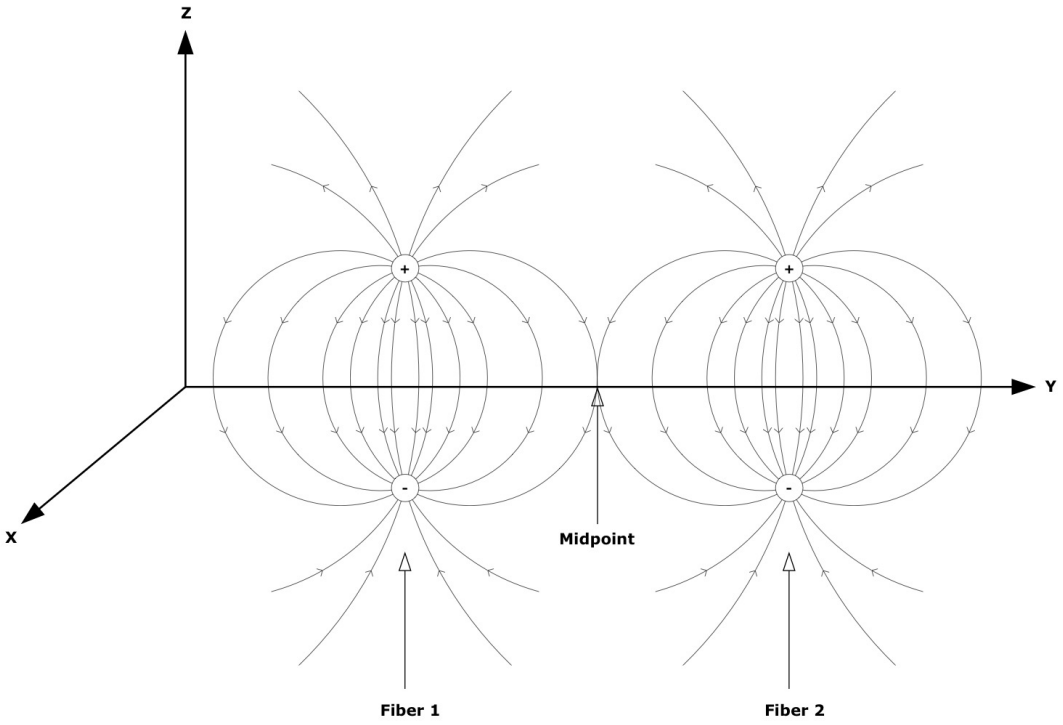

Figure 2.6: We choose the midpoint between two nanofibers to calculate the total electric field.

We plug equation (2.26) into equation (2.27) and the birefringence-magnetic field coupling equation would be

$$\begin{aligned} \Delta n &= (4.96 \times 10^{-7})[\tfrac{(1\times 10^6)\alpha_{33}^{*\,2}(V_1+V_2)^2}{\pi^4 {\epsilon_0}^2 d^6} H^2] + 5.12 \times 10^{-4} \\ &= \tfrac{0.496\alpha_{33}^{*\,2}(V_1+V_2)^2}{\pi^4 {\epsilon_0}^2 d^6} H^2 + 5.12 \times 10^{-4} \\ &= \beta H^2 + 5.12 \times 10^{-4}, \end{aligned} \tag{2.28}$$

where the coupling constant $\beta \equiv \frac{0.496\alpha_{33}^{*\,2}(V_1+V_2)^2}{\pi^4 {\epsilon_0}^2 d^6}$.

2.2 Numerical results of PVK polymer

Since the volume ratio between both phases is 1 : 1 [1], the volume fraction of the magnetostrictive phase f is $\frac{1}{2}$. We plug the numerical values into the equation (2.21)

to get the effective magnetoelectric coefficient as

$$\alpha_{33}^{*} \simeq 2.78 \times 10^{-15}\ (s/\mu m). \tag{2.29}$$

Assume that two Janus nanofibers have the same volumes ($V = 1600\ \mu m^3$) and then we calculate the coupling constant as

$$\beta \simeq \frac{5.14 \times 10^{-3}}{d^6}\ (m^2/A^2). \tag{2.30}$$

Substituting the equation (2.30) into the equation (2.28), we obtain

$$\Delta n = \frac{5.14 \times 10^{-3}}{d^6} H^2 + 5.12 \times 10^{-4}. \tag{2.31}$$

From the equation (2.31), we understand that different distances between two nanofibers would affect the polymer birefringence. In Figure 2.7, the slope of red curve increases more rapidly than others. When applying an external magnetic field from 0 to 2500 Oe, the fourth digit after the decimal point of PVK birefringence can clearly be distinguished. Since our experiment can detect the birefringence variation of 1 part in 10^4 and falls off as $\frac{1}{d^6}$, it is critical for the fiber distribution that the distance between two nanofibers should be within 15 μm. Therefore, a distance of 15 μm is used in equation (2.31), and we obtain the equation of PVK birefringence as

$$\Delta n = (4.51 \times 10^{-10}) H^2 + 5.12 \times 10^{-4}. \tag{2.32}$$

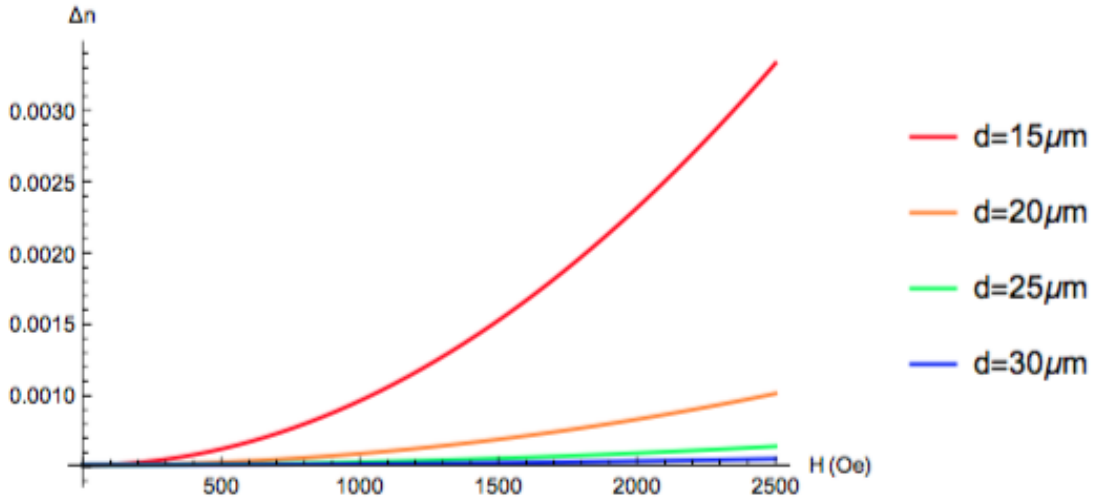

Figure 2.7: Birefringences of PVK polymer with distances varying from 15 μm to 30 μm.

2.3 Comparison with other polymers

In addition to PVK polymer, we know that $Poly(L-lactide)$ (P-L-LA), $Poly(D,L-lactide)$ (P-D,L-LA), and $Poly(ST-Na-AMPS)$ also display field-induced birefringence [7][8]. Here, we also use a distance between both nanofibers of 15 μm because we have obtained the numerical results in the previous section and would like to compare the differences among other polymers. The birefringences of these three kinds of polymers with different solute concentrations are shown in Table 2.2. Figure 2.8 shows that the birefringence change is only 1 part in 10^7 with magnetic field. The values are so small that we will not be able to detect them with our current experiment. Thus, P-L-LA and P-D,L-LA are not suitable polymers for us. In Figure 2.9, the slopes of curves for $Poly(ST-Na-AMPS)$ are negative, since the extraordinary index of refraction n_e is smaller than the ordinary index of refraction n_o. For the concentration $c = 6.87 \times 10^{-4} g/mL$, we predict that 1 part in 10^4 can be observed while varying the magnetic field. Therefore, both PVK and $Poly(ST-Na-AMPS)$ with

Table 2.2: Birefringences of $Poly(ST-Na-AMPS)$, P-L-LA, and P-D,L-LA with different concentrations.

Birefringence Δn	Polymer	Concentration c
Δn=$(1.24 \times 10^{-12})H^2$	P-L-LA	$c = 11.1 mg/cm^3$
Δn=$(1.07 \times 10^{-12})H^2$	P-L-LA	$c = 9.59 mg/cm^3$
Δn=$(6.53 \times 10^{-13})H^2$	P-L-LA	$c = 5.87 mg/cm^3$
Δn=$(5.15 \times 10^{-13})H^2$	P-L-LA	$c = 4.62 mg/cm^3$
Δn=$(2.70 \times 10^{-13})H^2$	P-L-LA	$c = 2.42 mg/cm^3$
Δn=$(2.45 \times 10^{-13})H^2$	P-L-LA	$c = 2.20 mg/cm^3$
Δn=$(5.16 \times 10^{-13})H^2$	P-D,L-LA	$c = 11.1 mg/cm^3$
Δn=$(4.46 \times 10^{-13})H^2$	P-D,L-LA	$c = 9.59 mg/cm^3$
Δn=$(2.73 \times 10^{-13})H^2$	P-D,L-LA	$c = 5.87 mg/cm^3$
Δn=$(2.15 \times 10^{-13})H^2$	P-D,L-LA	$c = 4.62 mg/cm^3$
Δn=$(1.13 \times 10^{-13})H^2$	P-D,L-LA	$c = 2.42 mg/cm^3$
Δn=$(1.02 \times 10^{-13})H^2$	P-D,L-LA	$c = 2.20 mg/cm^3$
Δn=$-(1.00 \times 10^{-9})H^2$	$Poly(ST-Na-AMPS)$	$c = 0.000687 g/mL$
Δn=$-(1.49 \times 10^{-10})H^2$	$Poly(ST-Na-AMPS)$	$c = 0.00126 g/mL$

the concentration $c = 6.87 \times 10^{-4} g/mL$ could enable a birefringence measurement.

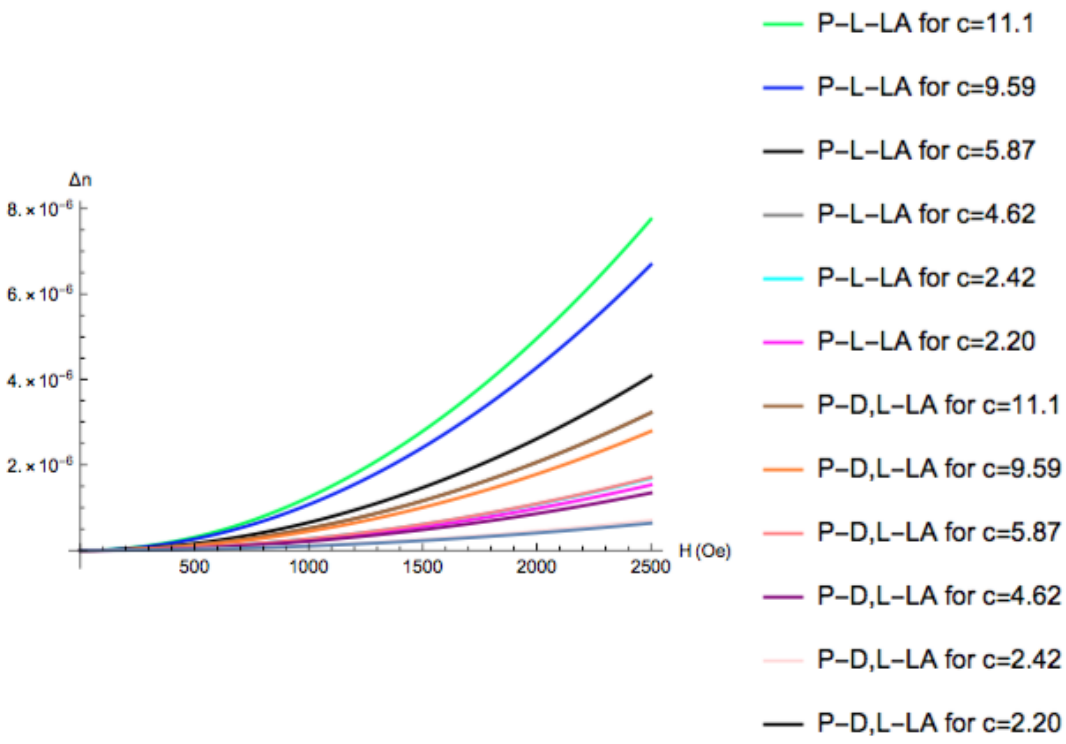

Figure 2.8: Birefringences of P-L-LA and P-D,L-LA polymers with different concentrations.

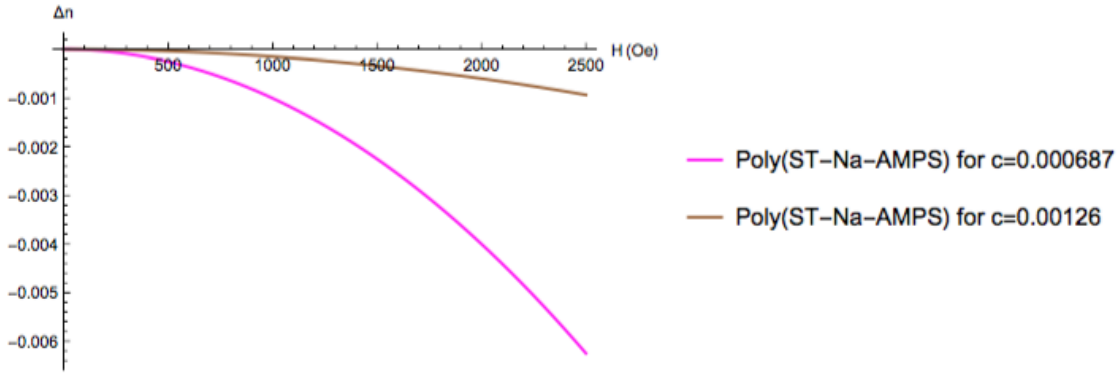

Figure 2.9: Birefringences of $Poly(ST - Na - AMPS)$ polymer with different concentrations.

Chapter 3

Experiment

3.1 Fabrication sample

In order to make the solution, we can put 1.5 mg Janus nanofibers into 6 ml PVK polymer liquid. Since the nanofibers can settle out in the container, the solution is mixed with a tip sonicator for 2 minutes. To avoid any dust on glass, we use a cotton swab with methanol to clean it first. A pipette is used to drop 50 μl solution on glass and put it on a spin coater with a speed of 450 rpm for 30 seconds to uniformly distribute the solution on the glass wafer. The sample is placed in an electromagnet with a high constant field to cure the sample for 1 hour. Then the nanofiber alignment and chaining experiment can be performed. The electric field from the piezoelectric phase can orient the PVK polymer along the specific direction by Kerr electro-optic effect. A microscope is then used to measure the polymer birefringence.

3.2 Birefringence measurement

In this experiment, we can use white light ($\lambda = 580nm$) to do the measurement. When the light passes through a polarizing material, it splits into two orthogonal rays called ordinary and extraordinary rays. This phenomenon is called birefringence [9]. Ordinary rays have a refractive index given by Snell's law, while extraordinary rays do not obey Snell's law. Thus, a birefringence measurement obtains the difference between the extraordinary and ordinary refractive indices. PVK polymer is chosen in

our research because it has this property of field-induced birefringence.

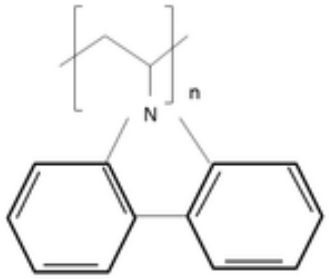

Figure 3.1: PVK chemical structure [by Sketchc89 from Wikipedia].

Once PVK polymer is oriented by the electric field mentioned in the previous section, the Carbon-Carbon (C-C) bond in PVK (Figure 3.1) forms as a long chain. The refractive index depends on the polarizability of this chemical bond [9]. When the polarized light enters the polymer, the speed of light perpendicular to C-C bond goes slower than the parallel part. We know that the refractive index is

$$n = \frac{c}{v}, \tag{3.1}$$

where c is speed of light in vacuum and v is speed of light in media. The birefringence is thus written as

$$\Delta n = n_{\parallel} - n_{\perp}, \tag{3.2}$$

where $n_{\parallel}$ and $n_{\perp}$ represent the refractive indices for light travelled parallel and perpendicular to the direction of orientation. The phase shift between both orthogonal beams is

$$\delta = \frac{2\pi \Delta n d}{\lambda}, \tag{3.3}$$

where d is the thickness of sample and λ is the wavelength of light.

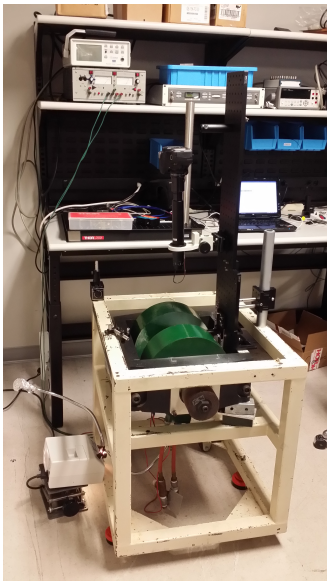

(a) Photo.

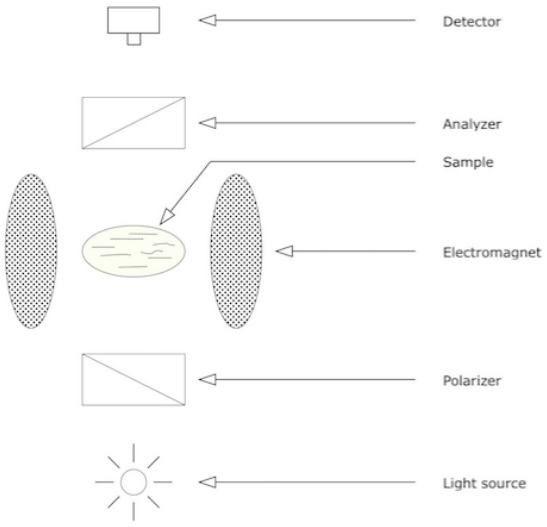

(b) Illustration.

Figure 3.2: Microscope setup.

The microscope is shown in Figure 3.2. First, we apply a constant magnetic field to cure the sample and orient the PVK polymer. In Figure 3.3, a polarizer is used to produce the polarized light from white light. Since the polarizer is set at an angle θ relative to the polymer orientation, the polarized light can be rotated by the sample. The light then passes through the analyzer which is perpendicular to the polarizer and a fraction of the light is transmitted through the analyzer. We use a Charge-Coupled Device (CCD) to collect these transmitted rays and analyze the intensity of light.

The light intensity I for birefringence measurement is

$$I = I_0 \sin^2(2\theta) \sin^2(\frac{\delta}{2}), \tag{3.4}$$

where I_0 is the initial light intensity produced from polarizer.

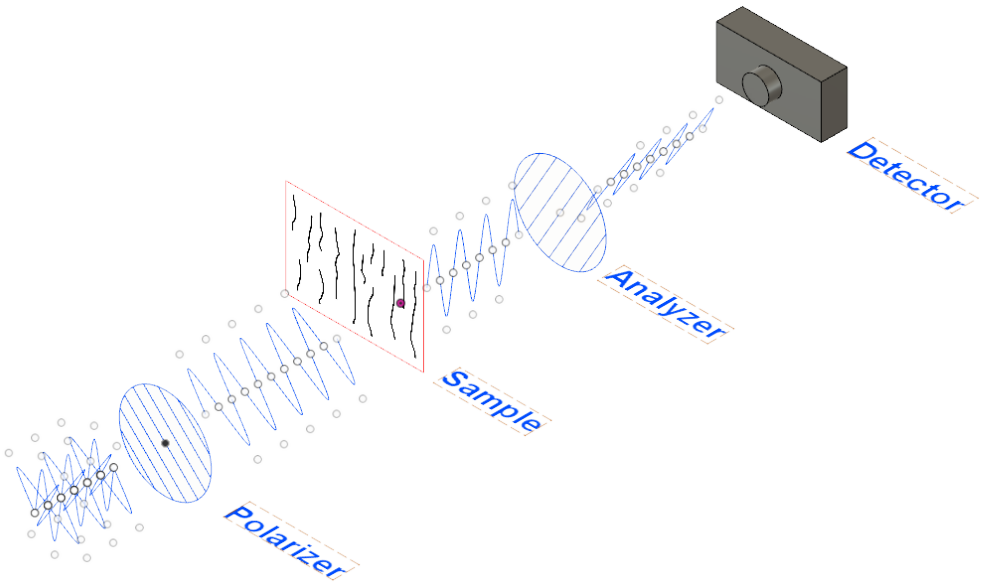

Figure 3.3: Polarized light microscopy.

3.3 Simulation and data analysis

The structure of polymer can create two orthogonal beams with a relative phase shift, and Table 3.1 shows these phase shifts in the polymer film for external magnetic fields ranging from 0 to 2500 Oe. We put these values into the equation (3.4) and obtain the angle-light intensity plots in Figure 3.4. As shown in Figure 3.4, the sinusoidal curves oscillate between 0 and a maximum value of light intensity while adjusting the angles of polarizer and analyzer to detect light intensity vs. magnetic fields. The data simulation can help us predict the experimental data quantitatively if we follow the sample making process and procedure of birefringence measurement mentioned in Sections 3.1 and 3.2 to do an experiment by our microscope.

Table 3.1: Phase shifts.

H (Oe)	δ (degrees)	$sin^2(\frac{\delta}{2})$
0	247.88	0.688285
250	261.53	0.573622
500	302.50	0.231385
750	370.77	0.00880083
1000	466.35	0.64071
1250	589.23	0.826496
1500	739.43	0.02847
1750	916.93	0.978326
2000	1121.74	0.126938
2250	1353.86	0.466299
2500	1613.29	0.996579

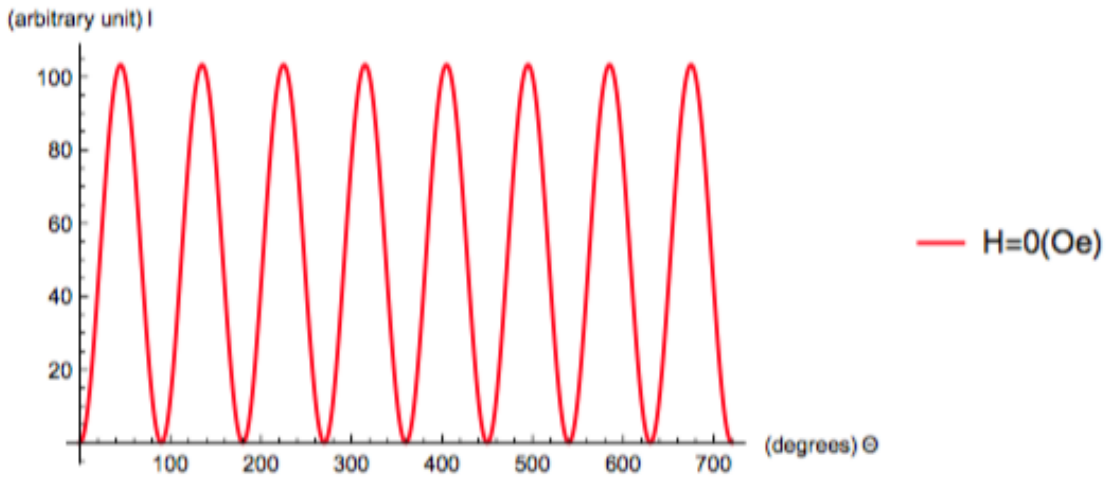

(a) θ - I plot for 0 Oe.

Figure 3.4: Polarizer angle θ - Light intensity I plots.

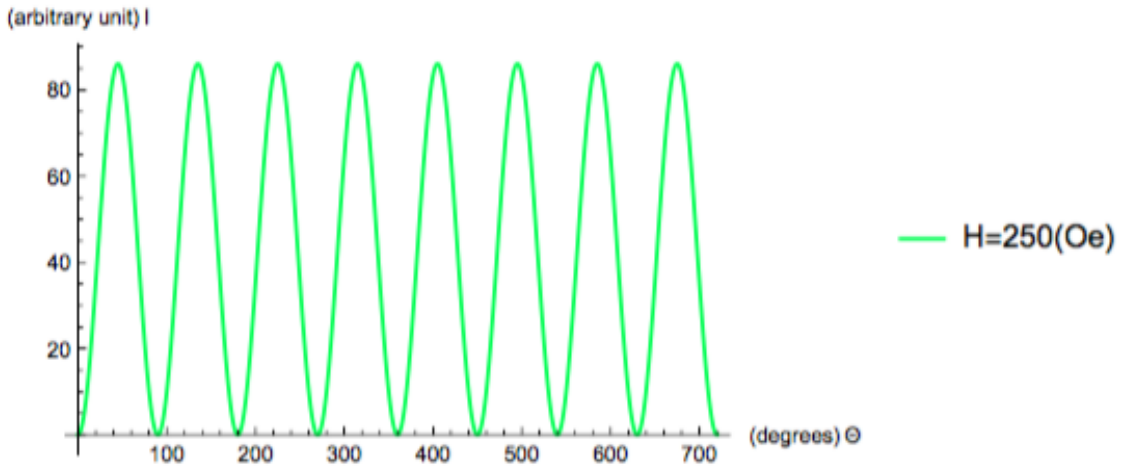

(b) θ - I plot for 250 Oe.

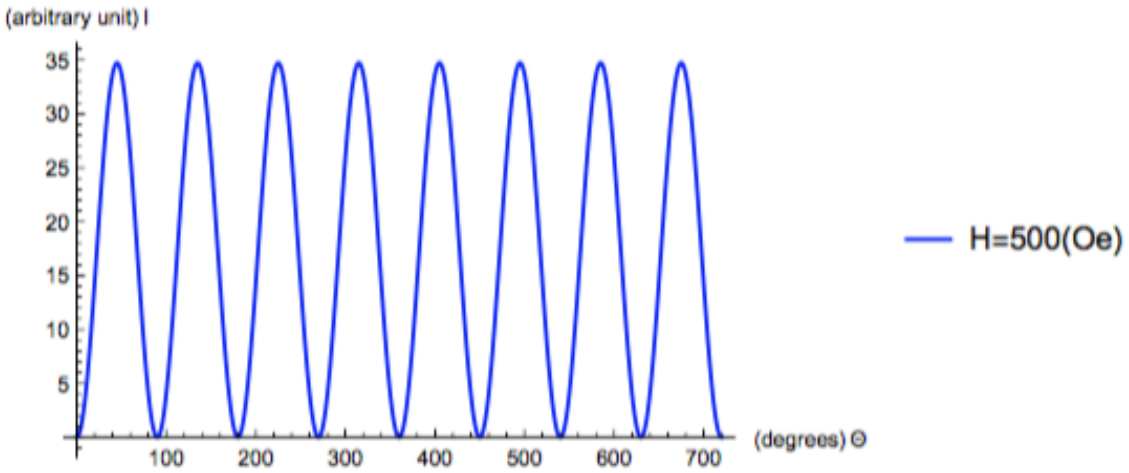

(c) θ - I plot for 500 Oe.

Figure 3.4: Polarizer angle θ - Light intensity I plots (cont.).

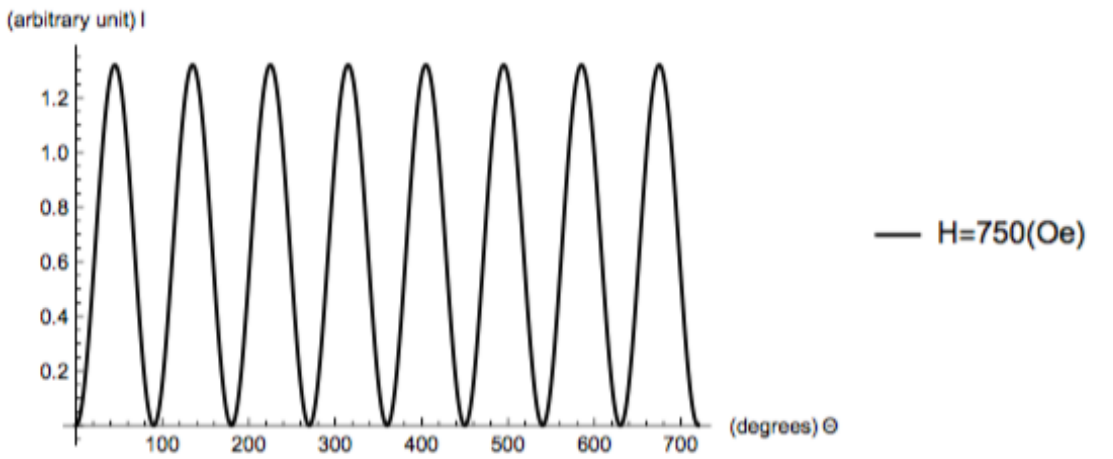

(d) θ - I plot for 750 Oe.

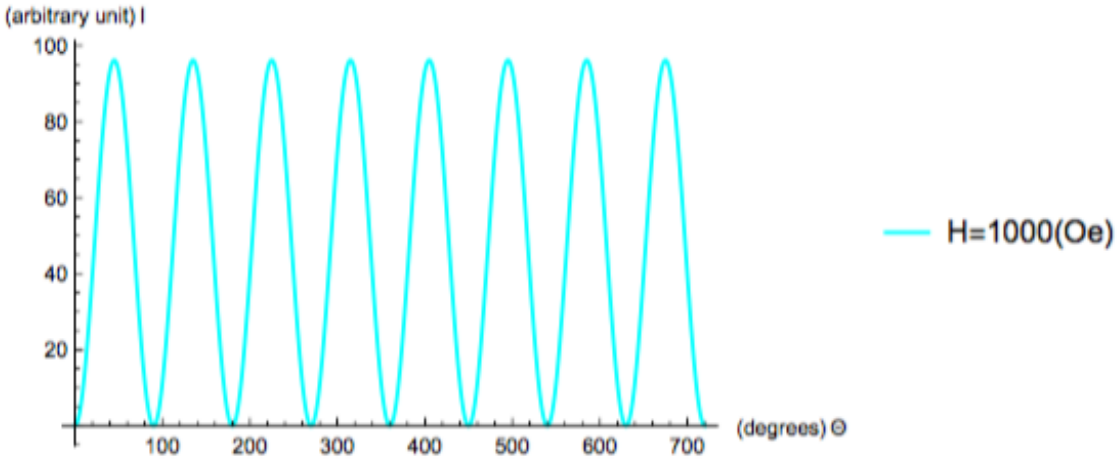

(e) θ - I plot for 1000 Oe.

Figure 3.4: Polarizer angle θ - Light intensity I plots (cont.).

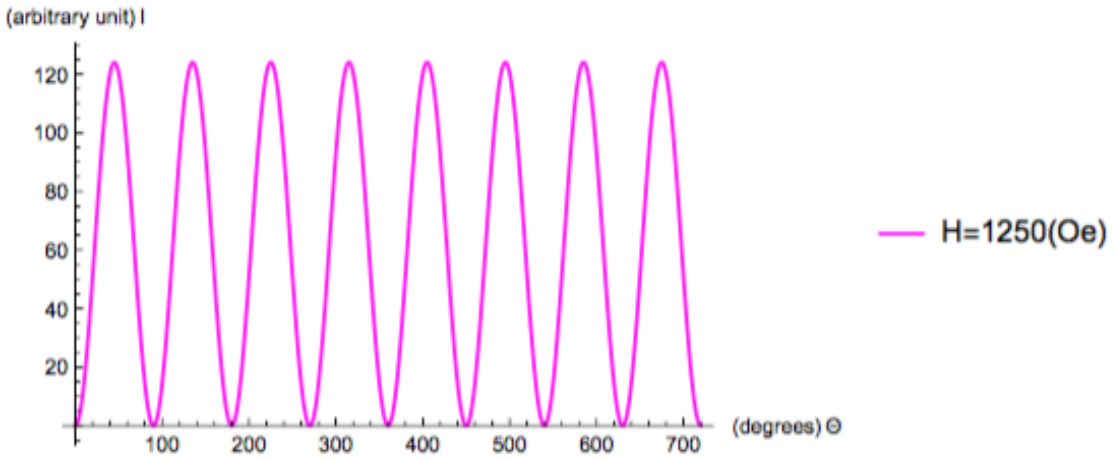

(f) θ - I plot for 1250 Oe.

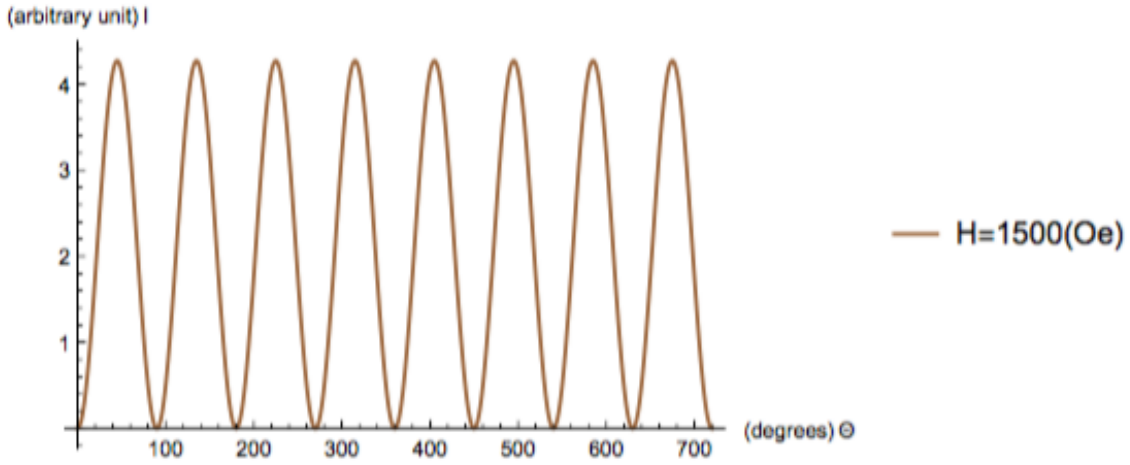

(g) θ - I plot for 1500 Oe.

Figure 3.4: Polarizer angle θ - Light intensity I plots (cont.).

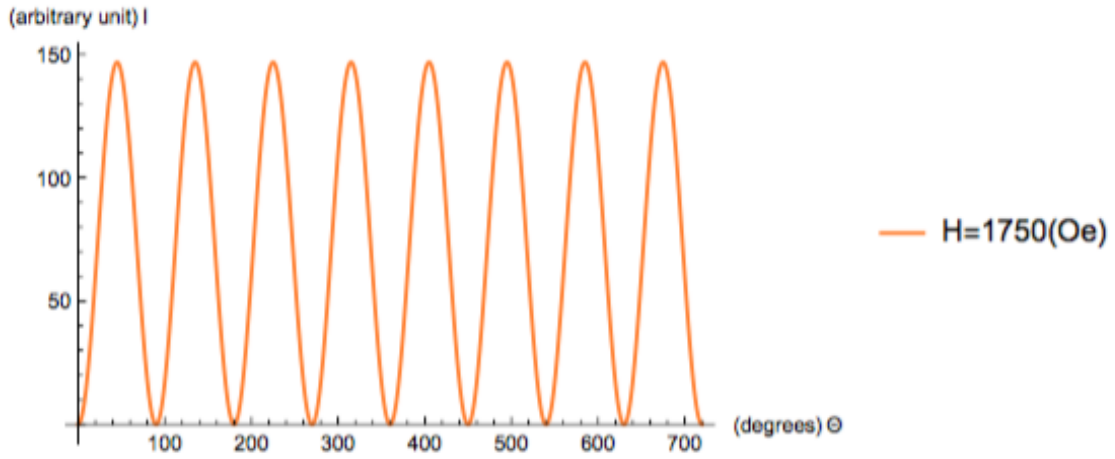

(h) θ - I plot for 1750 Oe.

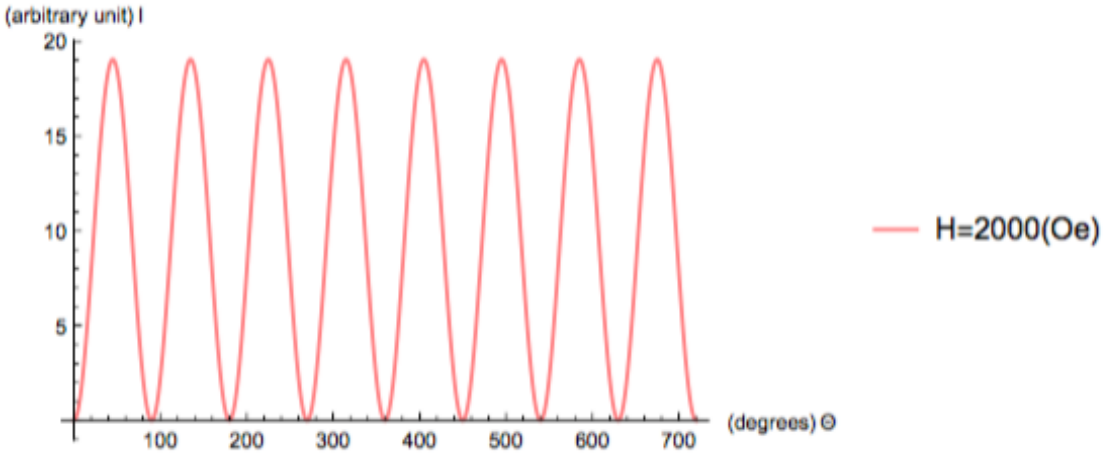

(i) θ - I plot for 2000 Oe.

Figure 3.4: Polarizer angle θ - Light intensity I plots (cont.).

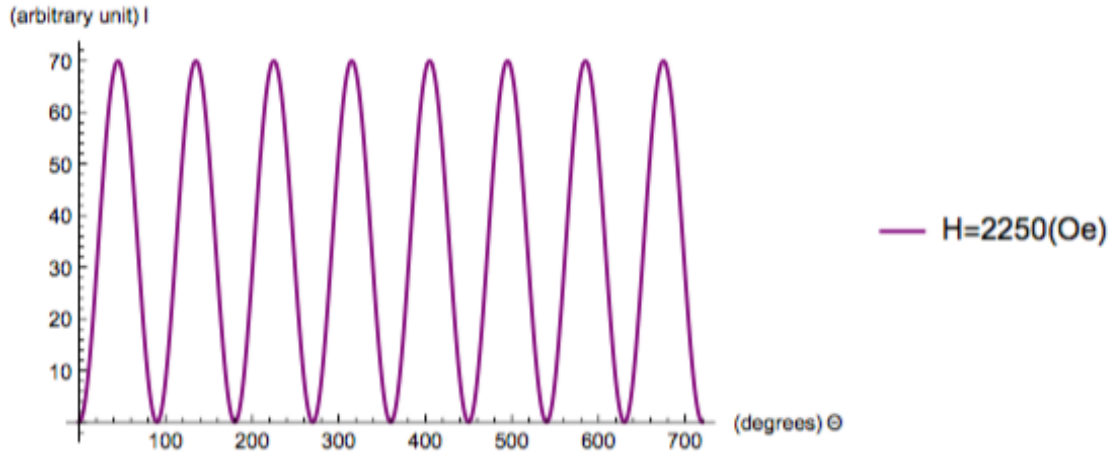

(j) θ - I plot for 2250 Oe.

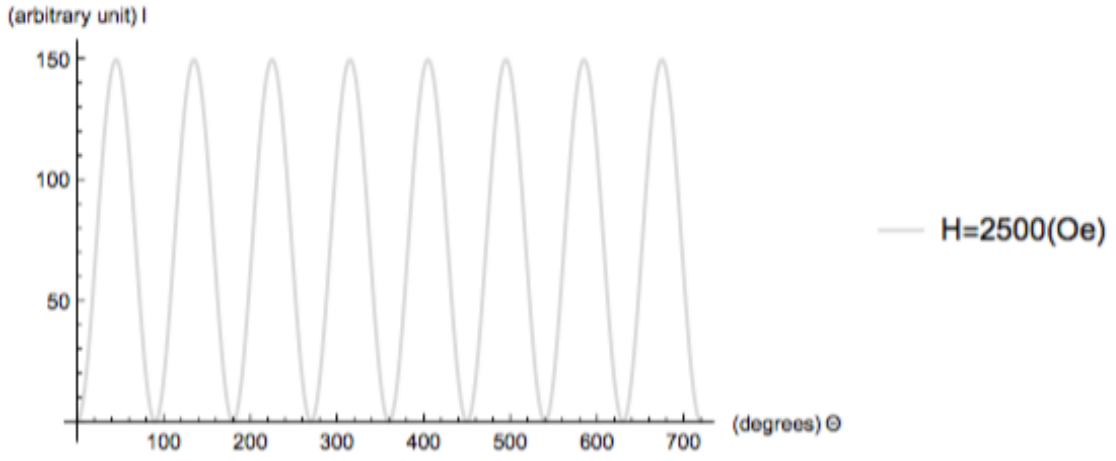

(k) θ - I plot for 2500 Oe.

Figure 3.4: Polarizer angle θ - Light intensity I plots (cont.).

Chapter 4

Conclusion and Future work

In this thesis, I have generalized the magnetic field-birefringence coupling equation from the magnetoelectric effect of Janus nanofibers and Kerr electro-optic effect of PVK polymer. Using the equation (2.32), I have shown that the distance between two fibers should be within 15 μm to obtain effective values of birefringence of PVK polymer that could be measured. Also, I found that $Poly(ST - Na - AMPS)$ with concentration $c = 6.87 \times 10^{-4} g/mL$ could be another option for a birefringence experiment. Future work involves making samples of PVK and $Poly(ST - Na - AMPS)$ with concentration $c = 6.87 \times 10^{-4} g/mL$ to observe the largest response for birefringence measurement. Then, we can compare experimental data with theoretical predictions and analyze the difference between them.

Bibliography

[1] Justin D. Starr and Jennifer S. Andrew, "*Janus-type bi-phasic functional nanofibers*," Chem. Commun., vol. 49, pp. 4151-4153, 2013.

[2] John D. Shakos, Mark D. Rahn, Dave P. West, and Kaleemullah Khand, "*Holographic index-contrast prediction in a photorefractive polymer composite based on electric-field-induced birefringence*," J. Opt. Soc. Am. B, vol. 17, iss. 3, pp. 373-380, 2000.

[3] Ce-Wen Nan, "*Magnetoelectric effect in composites of piezoelectric and piezomagnetic phases*," Phys. Rev. B, vol. 50, iss. 9, pp. 6082-6088, 1994.

[4] Ce-Wen Nan, "*Effective-medium theory of piezoelectric composites*," J. Appl. Phys., vol. 76, no. 2, pp. 1155-1163, 1994.

[5] Ce-Wen Nan, M. I. Bichurin, Shuxiang Dong, D. Viehland, and G. Srinivasan, "*Multiferroic magnetoelectric composites: Historical perspective, status, and future directions*," J. Appl. Phys., vol. 103, iss. 3, p. 031101, 2008.

[6] Ce-Wen Nan, "*Physics of inhomogeneous inorganic materials*," Prog. Mater. Sci., vol. 37, iss. 1, pp. 1-116, 1993.

[7] Georges M. Pavlov, Iliya V. Aver'yanov, Igor P. Kolomiets, Galina F. Kolbina, Olga A. Dommes, Olga V. Okatova, Victor A. Korzhikov, Anatoliy V. Dobrodumov, and Tatiana B. Tennikova, "*Conformational features of poly-L- and poly-D,L-lactides through molecular optics and hydrodynamics*," Eur. Polym. J., vol. 89, pp. 324-338, 2017.

[8] Zhulun Wang, Jian Wang, Benjamin Chu, and Dennis G. Peiffer, "*Solution Behavior of Random Copolymers of Styrene with Sodium-2-Acrylamido-2-Methylpropane Sulfonate*," J. Polym. Sci. B, vol. 29, iss. 11, pp. 1361-1371. 1991.

[9] "*The Theory of Birefringence*," URL: `http://www.campoly.com/files/4213/7122/7769/014_New_birefringence_theory.pdf`.